Progress In Electromagnetics Research Letters, Vol. 78, 73–79, 2018

A 28-GHz Antenna for 5G MIMO Applications

Zamir Wani, Mahesh P. Abegaonkar*, and Shiban K. Koul

Abstract—In this letter a four-port multi-input-multi-output (MIMO) antenna for 5G applications is proposed. This antenna is compact with a size of 11 mm × 31 mm excluding feed lines. The radiation patterns of the antenna show pattern diversity in the azimuthal plane, and each antenna element has an end-fire gain about 10 dBi by employing an array of metamaterial unit cells. The isolation between the antenna elements with edge to edge separation $< \lambda_0/5.5$ at 28 GHz is enhanced by trimming the corners of the rectangular high refractive index metamaterial region along with a ground stub between antennas. The proposed antenna is fabricated, and each antenna element has return loss, $S_{nn} < -10$ dB with isolation, $S_{nm} > 21$ dB in the frequency range 26 GHz to 31 GHz, which makes this antenna potential candidate for MIMO application at 28 GHz band enabling 5G cellular communications.

1. INTRODUCTION

28-GHz frequency band has emerged as potential candidates for next generation communication due to its low oxygen absorption rates unlike 60 GHz [1]. The mmWave MIMO technique is going to be the promising candidate to deliver high data rates required for streaming 8K video content and virtual reality services.

To counter the issues like high path loss and interference at 28-GHz, high gain antennas designed with MIMO and beamforming capabilities are proposed [2]. Various MIMO antennas for 5G applications have been proposed in [3–9]. In [10], a Ka-band MIMO antenna is proposed with a gain about 9.5–11 dBi and has a good isolation of 20 dB between the ports in the frequency range from 26.8 to 28.4 GHz, but this antenna occupies good amount of space (39.8 mm × 33.4 mm) on the board. In [11], the authors have managed to get isolation greater than 37.1 dB between two antipodal Fermi-based tapered slot antennas using metasurface corrugation in the frequency range 27 to 32 GHz on a 20 mil Rogers substrate ($\varepsilon_r = 3.55$) with only two antennas in an area 41 mm × 85 mm. Also a four-port MIMO antenna operating at 30 GHz is proposed in [12], and each port consists of an array of four dielectric resonator antennas (DRA) to have a gain of 10 dBi by feeding DRAs with microstrip lines, which results in significant losses at mmWave frequencies.

Mutual coupling between the antennas plays an important role in determining the performance of the MIMO communication network. Electromagnetic band-gap structure is proposed to reduce the coupling between antennas in [13]. In [14], single-negative magnetic metamaterials are employed to suppress the coupling between two monopole antennas. However, these techniques are not suitable for end-fire antennas. The authors in [15] have enhanced the isolation between two monopole antennas using an array of capacitively loaded loops (CLL) by about 10 dB.

In this letter, an mmWave MIMO antenna is designed, and each dipole antenna is loaded with a high refractive index CLL unit cell array. The loading of the CLL unit cell array serves two purposes: 1. This array acts as a high refractive index region; therefore, integration of CLL unit cell array with the dipole antennas enhances the gain of each to about 10 dBi and 2. Introducing defects (trimming) in

Received 3 July 2018, Accepted 19 August 2018, Scheduled 31 August 2018
* Corresponding author: Mahesh P. Abegaonkar (mpjosh@care.iitd.ac.in).
The authors are with the Centre for Applied Research in Electronics, Indian Institute of Technology Delhi, India.

the high refractive index metamaterial unit cell array reduces the mutual coupling between the closely spaced dipole antennas by about 10 dB at 30 GHz. The low mutual coupling between the antennas and each antenna having a good gain advocates the feasibility of this antenna for mmWave MIMO applications.

2. ANTENNA DESIGN

The two and four element antenna design for mmWave MIMO applications is discussed below in this section. The design process consists of two main aspects to address for mmWave: 1. Gain enhancement for high signal attenuation and 2. Isolation enhancement between the antenna elements, essential for spatial multiplexing. Starting with the two element dipole antenna configuration with improvement in isolation and then translating antennas to form four element MIMO configuration for better throughput of the communication network is discussed in this section.

2.1. Two Antenna MIMO Configuration

The proposed two element antenna configuration is designed on a Neltec substrate with dielectric constant, $\varepsilon_r = 2.2$, loss tangent $= 0.0009$ and height, $h = 10$ mil. The half wave dipole antenna designed using CST Microwave Studio software and fed with a microstrip line of width $w_i = 0.77$ mm has a gain about 5 dB at 28 GHz frequency, which is not desirable for communication at mmWave frequency band. High gain antenna design is very crucial, planar Yagi-Uda antennas are most popular end-fire antennas for their high gain [16]. Here to achieve a gain around 11 dBi, about 6–7 directors need to be placed which would considerably increase the size of the dipole antenna. Therefore, the gain of the dipole antenna is enhanced by placing the array of CLLs. The CLL-unit cell parameters shown in Fig. 1 are extracted from S-Parameters using [17] when being excited with PEC and PMC boundary conditions in x-direction and z-direction. This array of unit cells increases the refractive index of the substrate to about 2.1 (increase in refractive index $\sim 42\%$), and thus focusing of electric field (E-field) is observed. The gain of each dipole antenna is increased to about 10 dBi which is essential for countering propagation losses at 28 GHz frequency band. The gain enhancement of the dipole antenna using the loading of metamaterial unit cells is achieved in [18], and the gain of 11 dBi is reported for the dipole antenna.

The geometry of the proposed antenna with array of metamaterial unit cells is shown in Fig. 2. In our design, the metamaterial unit cell array is fed by two dipole antennas in MIMO configuration. The antennas are separated by a distance $S_{dd} = 1.9$ mm, and the mutual coupling between the ports due to surface waves is affected by adding a stub between the two antennas in the ground plane which introduces the resonance, and the surface current gets accumulated around the stub [19], resulting in enhancement of isolation between the ports. The isolation between the two antennas for different values of the stub length is shown in the Fig. 3(a). For a stub length of $l_{sb} = 1.8$ mm, which is $\lambda/4$ at 28 GHz,

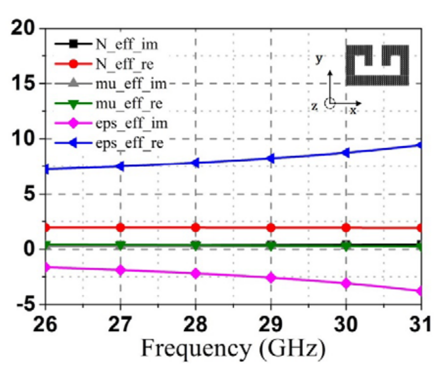

Figure 1. Extracted real part (re) and imaginary part (im) of refractive index (N), effective permittivity (eps) and permeability (mu) from S-parameters.

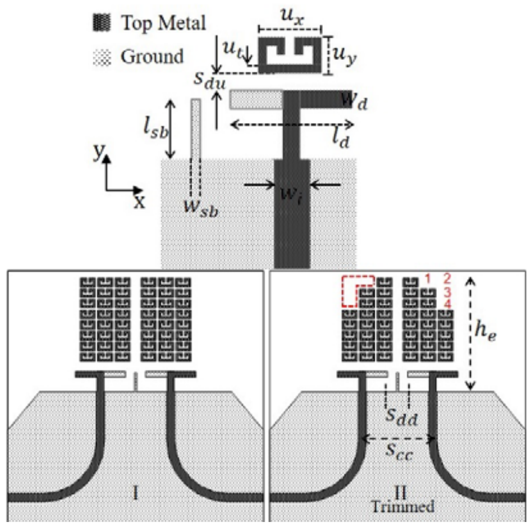

Figure 2. Geometry of two element MIMO antenna with array of unit cells. Zoomed view of dipole and unit cell along with Case-I: without trimming and Case-II: with trimming of corners. ($S_{cc} = 5.8$, $S_{dd} = 1.9$, $w_i = 0.77$, $h_e = 10.7$, $l_d = 4.7$, $w_d = 0.5$, $w_{sb} = 0.2$, $l_{sb} = 1.8$, $u_t = 0.2$, $s_{du} = 1.2$, $u_x = 1.4$, $u_y = 0.8$, all dimensions in millimeters).

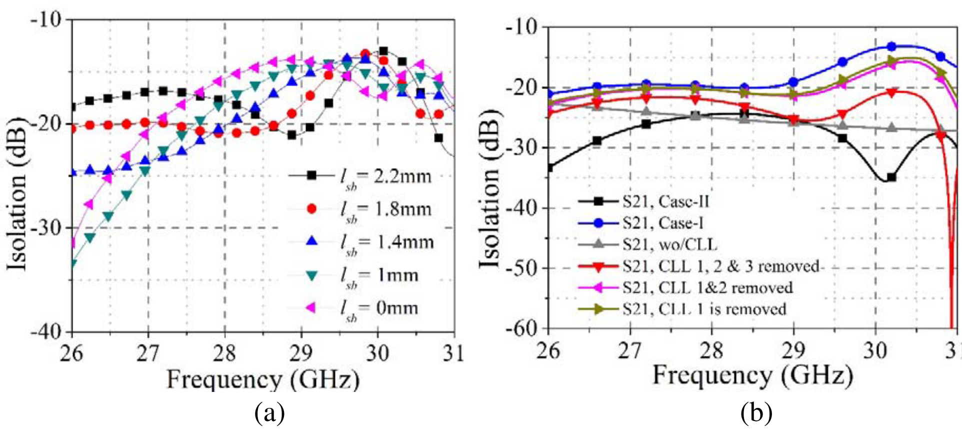

Figure 3. Isolation between dipole antennas (a) as a function of stub length (l_{sb}), (b) without corner trimming (Case I), with corner trimming (Case II), without any CLL array (wo/CLL) and if individual CLL unit cells are removed.

the isolation at 28 GHz is increased to 20 dB from 15 dB when a stub is added to the ground.

The other component of the mutual coupling is due to the spatial fields propagating to adjacent antenna through the CLL array. This coupling between the ports is seen dependent upon the coupling of the H-field (displacement current) from the high refractive region on the left (if port 1 is fed) to excite the array on right, which then propagates back through the CLL array to the adjacent dipole antenna. The effectiveness of trimming of the CLL array is investigated, and parametric analysis is done by removing the CLL unit cells. The isolation between the antennas for Case I — without trimming, Case II — with trimming and by removing CLL-1, 2 and 3 is shown in Fig. 3(b), which shows an improvement of 5 dB (at 28 GHz and 10 dB at 30 GHz) in isolation, and the overall isolation is greater than 25 dB in the whole frequency band for Case-II. Fig. 4 shows how the isolation is improved by mitigating the displacement current by trimming the top corners on right and left of high refractive index region. The coupling of current can be seen from the CLL array on the right for Case-I (if port 1 is fed), when no trimming is done.

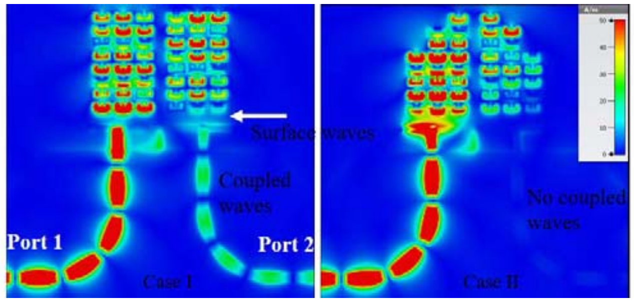

Figure 4. Snapshot of the H-filed in XY-Plane depicting the mutual coupling between the antennas when Port 1 is fed for the Case-I and Case-II at 30 GHz.

2.2. Four Antenna MIMO Configuration

The proposed four port MIMO antenna configuration is shown in the Fig. 5. All the four antennas are printed on a 10 mil Neltec substrate. The dipole antennas are separated by $S_{cc} = 6$ mm in x-direction and by $S_{hd} = 2.2$ mm along y-direction. All the four antennas and the metamaterial loading to enhance the gain cover a space of $1.05\lambda_{\mathbf{0@28\,GHz}} \times 2.9\lambda_{\mathbf{0@28\,GHz}}$ on the substrate without feeds, and feed lines are extended so as to accommodate the end-launch connectors. Each antenna is fed by a 50 ohm microstrip line, and the dipole antenna radiates along the y-direction. The E-field is focused by the array of metamaterial unit cells in different directions depending upon which of the antennas is fed.

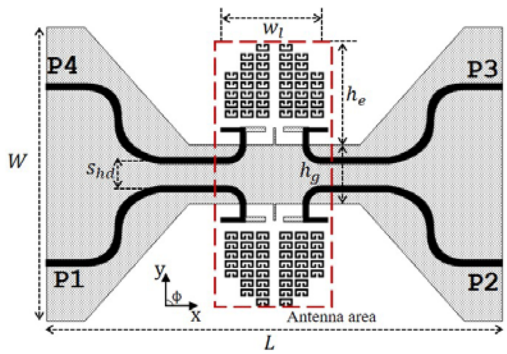

Figure 5. Proposed four port MIMO antenna configuration geometry. ($W = 31$, $L = 48$, $w_l = 10.4$, $h_e = 10.7$, $h_g = 6.2$, $S_{hd} = 2.2$, dimensions in mm).

3. EXPERIMENTAL RESULTS

The proposed four port antenna for MIMO applications at 28 GHz frequency band is fabricated in-house using the lithography process. The 2.92 mm End Launch Connectors from Southwest Microwave, Inc. are used for measuring the port performance of the prototype antenna shown in Fig. 6(a) using Keysight PNA in our lab. The radiation performance of the antenna is characterized in an anechoic chamber (far-field type) facility available in our Centre, and the setup is shown in Fig. 6(a).

The measured and predicted spectral performance of the 4-port antenna is analyzed. The return loss for all ports of the antenna in the frequency range 26 GHz to 31 GHz is shown in Fig. 6(b), and the return loss is well below $S_{nn} < -10$ dB. The isolation between the antenna elements is given in Fig. 6(c). This is a very important parameter for the MIMO antennas at 28-GHz, because high isolation (low coupling) between the ports will result in an enhanced efficiency of the individual elements. In addition, it will reduce the power loss due to coupling. Also the high isolation between antennas makes them independent so that high diversity gains can be achieved. The isolation between the ports $S_{nm} > 21$ dB is good enough for MIMO applications at 28 GHz band in such a small space. The radiation pattern of

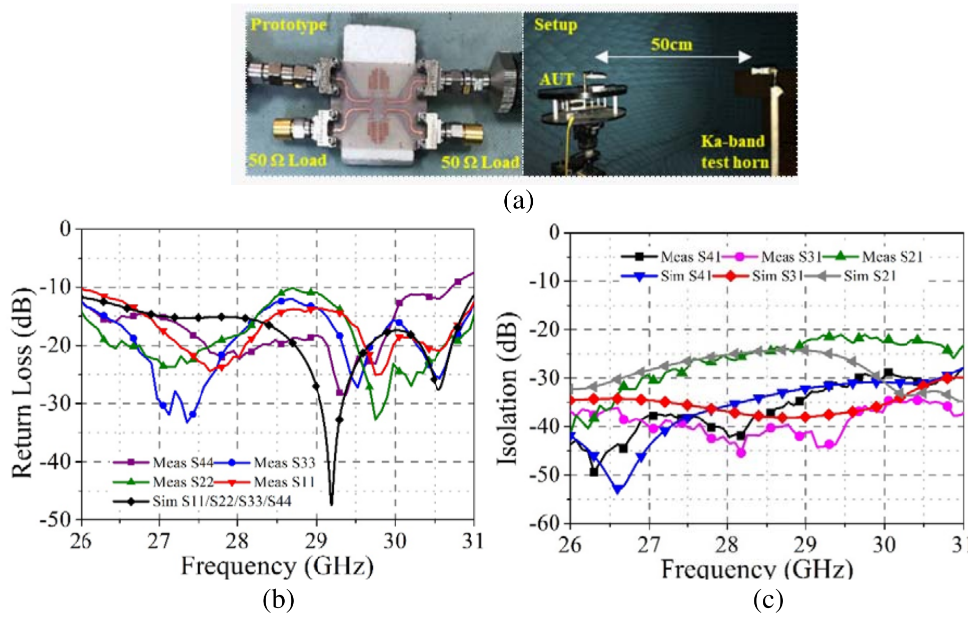

Figure 6. Port performance of the antenna. (a) Photograph of the prototype antenna and measurement setup, (b) measured and simulated return loss and (c) measured and simulated isolation.

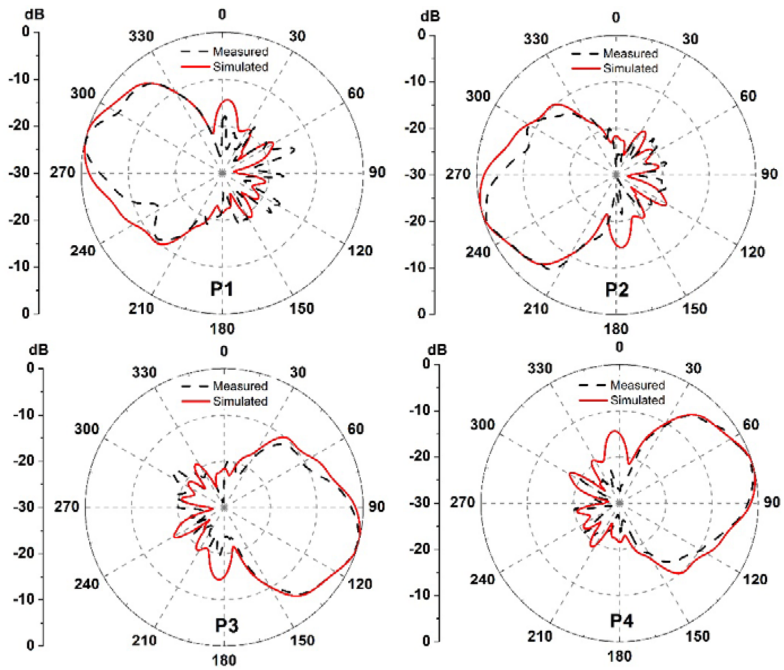

Figure 7. Measured and simulated normalized gain patterns in XOY-plane at 28 GHz when different ports are excited (Red: Simulated, Black: Measured).

the antenna at 28 GHz for four ports when other ports are terminated with 50 ohm in the XY-plane is shown in Fig. 7. The gain patterns show pattern diversity at 28 GHz when being excited at different ports, and the patterns are stable across the band. As the gains of all antennas are the same, only the measured and simulated gains of the antenna1 are plotted in Fig. 8 for the frequency band. It is evident from the figure that the dipole antenna with CLL array has a stable gain about 10 dBi in the frequency band.

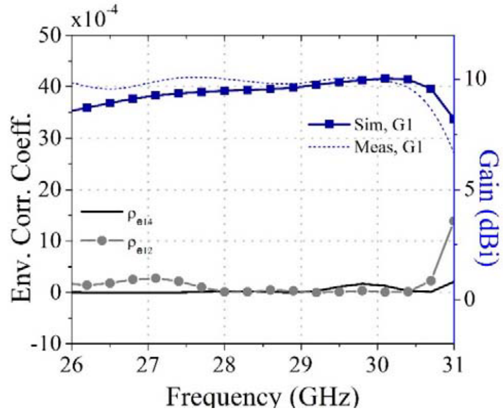

Figure 8. Envelope correlation coefficient between ports 1&2, 1&4 and gain of the antenna element 1 vs frequency.

The MIMO performance of the antenna is evaluated using the parameter envelope correlation coefficient (ECC or ρ_e), which determines the diversity gain of the multiple antenna systems [20]. The diversity gain will be high for small values of ρ_e, which results in improved system performance. The ECC is plotted between antenna elements 1 and 2 (ρ_{e12}) and between antenna elements 1 and 4 (ρ_{e14}) in Fig.? 7. The value of ECC is calculated using far-field results in the CST MWS and is well below 15×10^{-4} in the entire frequency band.

The proposed antenna is characterized. The performance is compared with the existing literature and presented in Table 1. The edge to edge distance between antenna elements is very small ($\lambda_0/6$) with a reasonably good isolation between the ports. To the best of our knowledge, the proposed four port antenna (without extended feed lines) is smaller than most of the reported MIMO antennas at 28 GHz frequency band.

Table 1. Comparison of the proposed work with other works.

Ref.	[3]	[5]	[11]	Proposed
Total size (mm^2)	48×21	NA	42×85	48×31
Operating band (GHz)	29.7–31.5	31–40.3	27–32	26-31
Min Isolation (dB)	25	21	37.1	21
Peak gain (dBi)	8.6	11	17.9	10
Edge to edge spacing (λ_0)	$\lambda_0/3.6$	$\lambda_0/1.27$	N/A	$\lambda_0/6$
Number of ports	2	4	2	4

λ_0 = free space wavelength at lowest operating frequency

4. CONCLUSION

A millimeter-wave antenna consisting of four dipole antenna elements is proposed for MIMO applications at 28 GHz band. The four port antenna has pattern diversity in XY-plane with each antenna offering gain of 10 dBi. All the four antennas occupy an area of $3\lambda_0^2$, (λ_0 = free space wavelength at 28 GHz) on the substrate without feeds while achieving a good isolation between the antennas. This compact antenna can be useful for 5G MIMO applications in a compact handheld device.

REFERENCES

1. Rappaport, T. S., J. N. Murdock, and F. Gutierrez, "State of the art in 60-GHz integrated circuits and systems for wireless communications," *Proc. IEEE*, Vol. 99, No. 8, 1390–1436, Aug. 2011.
2. Yang, B., Z. Yu, Y. Dong, J. Zhou, and W. Hong, "Compact tapered slot antenna array for 5G millimeter-wave massive MIMO systems," *IEEE Trans. Antennas Propag.*, Vol. 65, No. 12, 6721–6727, Dec. 2017.

3. Sharawi, M. S., S. K. Podilchak, M. T. Hussain, and Y. M. M. Antar, "Dielectric resonator based MIMO antenna system enabling millimetre-wave mobile devices," *Antennas Propag. IET Microw.*, Vol. 11, No. 2, 287–293, 2017.
4. Sharawi, M. S., M. Ikram, and A. Shamim, "A two concentric slot loop based connected array MIMO antenna system for 4G/5G terminals," *IEEE Trans. Antennas Propag.*, Vol. PP, No. 99, 1–1, 2017.
5. Hsu, Y. W., T. C. Huang, H. S. Lin, and Y. C. Lin, "Dual-polarized quasi Yagi-Uda antennas with endfire radiation for millimeter-wave MIMO terminals," *IEEE Trans. Antennas Propag.*, Vol. 65, No. 12, 6282–6289, Dec. 2017.
6. Sharma, A., A. Sarkar, M. Adhikary, A. Biswas, and M. J. Akhtar, "SIW fed MIMO DRA for future 5G applications," *2017 IEEE International Symposium on Antennas and Propagation USNC/URSI National Radio Science Meeting*, 1763–1764, 2017.
7. Ikram, M., M. S. Sharawi, A. Shamim, and A. Sebak, "A multiband dual-standard MIMO antenna system based on monopoles (4G) and connected slots (5G) for future smart phones," *Microw. Opt. Technol. Lett.*, Vol. 60, No. 6, 1468–1476, Jun. 2018.
8. Parchin, N. O., M. Shen, and G. F. Pedersen, "End-fire phased array 5G antenna design using leaf-shaped bow-tie elements for 28/38 GHz MIMO applications," *2016 IEEE International Conference on Ubiquitous Wireless Broadband (ICUWB)*, 1–4, 2016.
9. Selvaraju, R., M. H. Jamaluddin, M. R. Kamarudin, J. Nasir, and M. H. Dahri, "Complementary split ring resonator for isolation enhancement in 5G communication antenna array," *Progress In Electromagnetics Research C*, Vol. 83, 217–228, 2018.
10. Lin, M., P. Liu, and Z. Guo, "Gain-enhanced Ka-band MIMO antennas based on the SIW corrugated technique," *IEEE Antennas Wirel. Propag. Lett.*, Vol. 16, 3084–3087, 2017.
11. Gupta, S., Z. Briqech, A. R. Sebak, and T. A. Denidni, "Mutual-coupling reduction using metasurface corrugations for 28 GHz MIMO applications," *IEEE Antennas Wirel. Propag. Lett.*, Vol. 16, 2763–2766, 2017.
12. Hussain, M. T., M. S. Sharawi, S. Podilchack, and Y. M. M. Antar, "Closely packed millimeter-wave MIMO antenna arrays with dielectric resonator elements," *2016 10th European Conference on Antennas and Propagation (EuCAP)*, 1–4, 2016.
13. Al-Hasan, M. J., T. A. Denidni, and A. R. Sebak, "Millimeter-wave compact EBG structure for mutual coupling reduction applications," *IEEE Trans. Antennas Propag.*, Vol. 63, No. 2, 823–828, Feb. 2015.
14. Bait-Suwailam, M. M., M. S. Boybay, and O. M. Ramahi, "Electromagnetic coupling reduction in high-profile monopole antennas using single-negative magnetic metamaterials for MIMO applications," *IEEE Trans. Antennas Propag.*, Vol. 58, No. 9, 2894–2902, Sep. 2010.
15. Sharawi, M. S., A. B. Numan, and D. N. Aloi, "Isolation improvement in a dual-band dual-element MIMO antenna system using capacitively loaded loops," *Progress In Electromagnetics Research*, Vol. 134, 247–266, 2013.
16. Alhalabi, R. A. and G. M. Rebeiz, "High-gain Yagi-Uda antennas for millimeter-wave switched-beam systems," *IEEE Trans. Antennas Propag.*, Vol. 57, No. 11, 3672–3676, Nov. 2009.
17. Szabo, Z., G. H. Park, R. Hedge, and E. P. Li, "A unique extraction of metamaterial parameters based on kramers kronig relationship," *IEEE Trans. Microw. Theory Tech.*, Vol. 58, No. 10, 2646–2653, Oct. 2010.
18. Wani, Z., M. P. Abegaonkar, and S. K. Koul, "Gain enhancement of millimeter wave antenna with metamaterial loading," *2017 International Symposium on Antennas and Propagation (ISAP)*, 1–2, 2017.
19. Wani, Z. and D. K. Vishwakarma, "An ultrawideband antenna for portable MIMO terminals," *Microw. Opt. Technol. Lett.*, Vol. 58, No. 1, 51–57, Jan. 2016.
20. Sharawi, M. S., "Current misuses and future prospects for printed multiple-input, multiple-output antenna systems [wireless corner]," *IEEE Antennas Propag. Mag.*, Vol. 59, No. 2, 162–170, Apr. 2017.